As per UGC guidelines an electronic bar code is provided to secure your paper

International Journal for Modern Trends in Science and Technology
Volume 11, Issue 02, pages 84-92.
ISSN: 2455-3778 online
Available online at: http://www.ijmtst.com/vol11issue02.html
DOI: https://doi.org/10.46501/ijmtst.v11.i02.pp84-92

Analysis of Tensile and Hardness Properties of Aluminum-Based Alloys

Dr. K. Chandra Sekhar

Associate Professor, Department of Mechanical Engineering, QIS College of Engineering and Technology, Ongole, Prakasam (Dt), Andhra Pradesh, INDIA.
Email: sekharc333@gmail.com

To Cite this Article
Dr. K. Chandra Sekhar, "Analysis of Tensile and Hardness Properties of Aluminum-Based Alloys", International Journal for Modern Trends in Science and Technology, 2025, 11(02), pages. 84-92. https://doi.org/10.46501/ijmtst.v11.i02.pp84-92

Article Info
Received: 12 January 2025; Accepted: 03 February 2025; Published: 14 February 2025.

ABSTRACT

Aluminum-based alloys are among the most widely used structural materials in the automotive, aerospace, marine, and general engineering sectors because of their high strength-to-weight ratio, good corrosion resistance, and excellent formability. The present work experimentally analyses the tensile and hardness properties of four commonly used aluminum alloys — Al 6061, Al 7075, Al 2024, and the cast alloy A356 — and examines how silicon-carbide (SiC) particulate reinforcement and T6 heat treatment influence these properties. Tensile tests were carried out on a universal testing machine using flat specimens prepared in accordance with ASTM E8, and hardness was measured using the Brinell and Vickers methods. Among the materials studied, Al 7075-T6 exhibited the highest ultimate tensile strength (≈ 572 MPa) and hardness (≈ 150 BHN), whereas Al 2024 offered the greatest ductility and A356 the lowest strength. The addition of SiC to an Al 6061 matrix progressively increased the tensile strength and hardness while reducing the elongation, and T6 heat treatment nearly doubled the strength and substantially raised the hardness of the as-cast alloy. A strong positive correlation was observed between hardness and ultimate tensile strength. The results confirm that the mechanical performance of aluminum-based alloys is governed primarily by alloy chemistry, reinforcement content, and thermal processing, and they provide useful guidance for material selection in lightweight structural applications.

KEYWORDS: Aluminum-based alloys, Tensile strength, Hardness, Yield strength, Ductility, ASTM E8, Brinell hardness, SiC metal-matrix composite, Heat treatment (T6), Strengthening mechanisms, Mechanical characterization.

NOMENCLATURE

σ engineering stress (MPa)

ε engineering strain (–)

F applied tensile load (N)

A_0 original cross-sectional area (mm^2)

L_0, L_f original and final gauge length (mm)

UTS ultimate tensile strength (MPa)

YS yield strength (MPa)

BHN Brinell hardness number

HV Vickers hardness

d average grain size (µm)

k Hall–Petch coefficient

V_m, V_r volume fraction of matrix, reinforcement

1. INTRODUCTION

Aluminum and its alloys occupy a central position among lightweight structural materials. With a density roughly one-third that of steel, combined with good corrosion resistance, high thermal and electrical conductivity, and excellent formability and recyclability, aluminum-based alloys are extensively used in the automotive, aerospace, marine, railway, packaging, and construction industries. In transport applications in particular, the drive to reduce weight — and thereby fuel consumption and emissions — has made the high strength-to-weight ratio of aluminum alloys a decisive advantage over heavier ferrous materials [1,2].

Pure aluminum is soft and of low strength, so its engineering usefulness depends on alloying and on subsequent thermal and mechanical processing. The principal alloying additions — copper, magnesium, silicon, zinc, and manganese — give rise to the standard wrought (1xxx–8xxx) and cast alloy families, each tailored to particular combinations of strength, ductility, and corrosion resistance. The heat-treatable alloys (notably the 2xxx Al–Cu, 6xxx Al–Mg–Si, and 7xxx Al–Zn–Mg systems) develop their strength through precipitation hardening, whereas the cast Al–Si alloys such as A356 are valued for castability and are widely used for automotive components [2,5].

Wrought aluminum alloys are designated by a four-digit number in which the first digit identifies the principal alloying element, and the temper is indicated by a suffix — for example, T4 (solution treated and naturally aged) and T6 (solution treated and artificially aged). The temper has as large an effect on the mechanical properties as the alloy chemistry itself, since it controls the size, distribution, and coherency of the strengthening precipitates. A meaningful comparison of alloys must therefore specify the temper, and in the present work the commonly supplied tempers (6061-T6, 7075-T6, 2024-T4, and A356-T6) are used so that the data correspond to the materials encountered in practice.

Two of the most important mechanical properties for design are the tensile strength and the hardness. The tensile test yields the yield strength, the ultimate tensile strength (UTS), and the ductility (percentage elongation), which together describe the load-bearing capacity and the ability to absorb deformation before fracture. Hardness, measured rapidly and almost non-destructively, characterises resistance to localised plastic deformation and wear and is known to correlate closely with tensile strength. Because these properties depend strongly on composition, reinforcement, and heat treatment, their systematic measurement is essential for reliable material selection [6–8].

The four alloys examined in this work were chosen because each dominates an important application area. Al 6061 is the general-purpose structural alloy used for frames, pipes, and marine fittings; Al 7075 is the high-strength alloy of choice for aircraft structural members and highly stressed parts; Al 2024 is favoured in aerospace skins and fittings where damage tolerance matters; and the cast alloy A356 is widely used for automotive wheels, cylinder heads, and housings. A side-by-side measurement of their tensile and hardness behaviour under a common test procedure therefore offers directly comparable design data that are often scattered across different sources.

A further route to higher specific strength and stiffness is the incorporation of hard ceramic particles — silicon carbide (SiC), alumina (Al_2O_3), or boron carbide — to form aluminum metal-matrix composites (AMMCs). Particulate SiC reinforcement, commonly introduced by stir casting, raises the strength, hardness, and wear resistance of the matrix, although usually at the expense of ductility [3,11]. Understanding the trade-off between strengthening and embrittlement is therefore an important part of characterising aluminum-based materials.

In the present study the tensile and hardness properties of four widely used aluminum alloys — Al 6061, Al 7075, Al 2024, and the cast alloy A356 — are measured and compared. The effect of SiC particulate reinforcement (0–

15 wt%) on an Al 6061 matrix and the effect of T6 heat treatment on the as-cast alloy are also examined. The specific objectives are: (i) to determine and compare the stress–strain behaviour, UTS, yield strength, ductility, and hardness of the selected alloys; (ii) to quantify the influence of SiC content on strength and hardness; (iii) to evaluate the strengthening produced by T6 heat treatment; and (iv) to establish the correlation between hardness and tensile strength. The methodology, governing relations, results, and conclusions are presented in the sections that follow.

2. LITERATURE REVIEW

Miller and co-workers [4] reviewed the development of aluminum alloys for the automotive industry and showed how the choice between 5xxx, 6xxx, and 7xxx alloys is dictated by the required combination of strength, formability, and corrosion resistance. They emphasised that the 6xxx Al–Mg–Si alloys offer an attractive balance of moderate strength and good formability for body panels, while the higher-strength 7xxx alloys are reserved for structural members, a hierarchy reflected in the tensile data of the present study.

Rana, Purohit and Das [5] surveyed the influence of alloying elements on the microstructure and mechanical properties of aluminum alloys and composites. They reported that copper and zinc additions give the largest strength increments through precipitation hardening, magnesium and silicon provide intermediate strengthening in the 6xxx series, and that the resulting precipitates raise hardness in parallel with strength. These trends underpin the ranking of the alloys examined here.

Surappa [3] reviewed the processing and properties of aluminum-matrix composites and identified stir casting as the most economical route for incorporating SiC and Al_2O_3 particulates. The review reported substantial gains in hardness, stiffness, and wear resistance with increasing reinforcement content, accompanied by a reduction in ductility owing to particle clustering and the constraint of matrix flow — behaviour reproduced by the SiC composites in Section 5.

Sajjadi and co-authors [11] studied Al–Al_2O_3 composites produced by casting and found that both micro- and nano-sized particles increased the tensile strength and hardness of the matrix, with a generally monotonic rise up to a critical particle content beyond which clustering and porosity began to degrade the properties. Their results support the use of a moderate reinforcement fraction, consistent with the optimum suggested by the present data.

Kaufman [6] compiled extensive tensile, creep, and fatigue data for commercial aluminum alloys and tempers, providing the reference property ranges against which experimental measurements are commonly validated. The measured values reported in Section 5 fall within the ranges tabulated in that compilation, confirming the reliability of the test procedure.

The classical work of Hall [9] and Petch [10] established the inverse-square-root dependence of yield strength on grain size, while standard test methods ASTM E8 [7] and E10 [8] define the tensile and Brinell hardness procedures. Together these references provide the theoretical and procedural framework adopted in the present investigation; collectively, the literature shows that composition, grain size, reinforcement, and heat treatment are the dominant levers controlling the tensile and hardness behaviour of aluminum-based alloys.

Hassan and Gupta [12] examined the effect of reinforcement particle size on solidification-processed aluminum composites and reported that finer, well-dispersed particles give a larger strength and hardness increment than coarse particles at the same volume fraction, because finer particles produce more effective dislocation pinning and a more uniform load transfer. This observation explains why particle size and distribution, not merely the weight fraction, must be controlled during stir casting, and it informs the interpretation of the composite results in Section 5.5.

Standard texts on light alloys and mechanical metallurgy [13,14,16] further establish that the four strengthening mechanisms operative in aluminum — solid-solution strengthening, grain-size (Hall–Petch) strengthening, work hardening, and precipitation hardening — act together, and that their relative contributions shift with alloy family and temper. The experimental trends reported here can be understood consistently within this framework, and the present study adds quantitative tensile and hardness data for a directly comparable set of alloys, composites, and heat-treatment conditions.

3. MATERIALS AND EXPERIMENTAL METHODS

Four aluminum alloys were selected to represent the principal heat-treatable and cast families: Al 6061 (Al–

Mg–Si), Al 7075 (Al–Zn–Mg–Cu), Al 2024 (Al–Cu–Mg), and the cast alloy A356 (Al–Si–Mg). In addition, an Al 6061 matrix reinforced with 0, 5, 10, and 15 wt% of silicon-carbide particulate (average size ≈ 25 μm) was prepared to study the effect of reinforcement. The overall experimental sequence is shown in Fig. 1, and the nominal chemical compositions of the base alloys are given in Table 1.

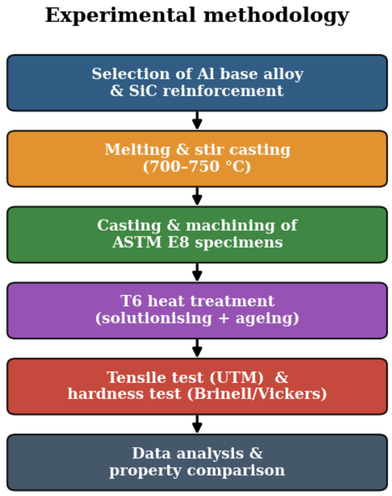

Fig. 1 Flow chart of the experimental methodology

Table 1: Nominal chemical composition (wt%) of the base aluminum alloys

Alloy	Si	Fe	Cu	Mn	Mg	Zn	Al
Al 6061	0.6	0.7	0.28	0.15	1.0	0.25	bal.
Al 7075	0.4	0.5	1.6	0.30	2.5	5.6	bal.
Al 2024	0.5	0.5	4.4	0.6	1.5	0.25	bal.
A356	7.0	0.20	0.20	0.10	0.35	0.10	bal.

3.1 Composite fabrication and specimen preparation

The SiC-reinforced composites were produced by the stir-casting route. The Al 6061 matrix was melted in a graphite crucible in an electric resistance furnace at about 720 °C; preheated SiC particles were added to the melt and dispersed using a mechanical stirrer rotating at roughly 400–500 rpm to obtain a uniform distribution, after which the melt was poured into a preheated permanent mould. Cast bars and the as-received wrought alloys were then machined into flat tensile specimens conforming to ASTM E8, with a 50 mm gauge length, as shown in Fig. 2. Hardness coupons were sectioned from the grip regions and surface-ground for testing.

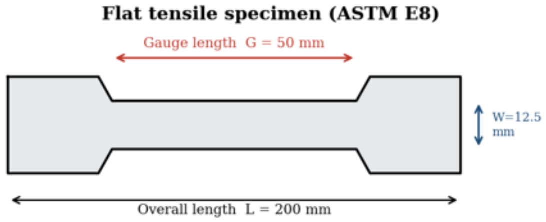

Fig. 2 Geometry of the flat tensile specimen (ASTM E8)

During stir casting, particular care was taken to promote wetting and uniform dispersion of the SiC particles, which is the chief difficulty of the route. The SiC powder was preheated to several hundred degrees to remove moisture and to improve wettability with the molten aluminium, and it was added gradually into the vortex created by the stirrer rather than all at once, so that the particles were drawn into the melt instead of floating on the surface. A short stirring period was maintained after the final addition to homogenise the slurry, and the melt was degassed before pouring to minimise gas porosity. These measures reduce particle clustering and casting defects, both of which would otherwise lower the strength and the reproducibility of the composite.

3.2 Tensile, hardness and heat-treatment procedures

Tensile testing was performed on a computerised universal testing machine (UTM) at a constant cross-head speed of about 1 mm/min at room temperature. The load–extension data were converted to engineering stress–strain curves, from which the yield strength (0.2% offset), UTS, and percentage elongation were obtained; three specimens were tested per condition and the mean values reported. Hardness was measured by the Brinell method (ASTM E10) using a 10 mm ball and a suitable load, with several indentations averaged per sample, and confirmed by Vickers micro-hardness on selected specimens. The T6 temper was produced by solution treatment near 530 °C followed by water quenching and artificial ageing, which develops the strengthening precipitates responsible for the increase in strength and hardness.

To ensure the reliability of the measurements, all specimens were prepared with the same surface finish and gauge geometry, and the testing machine was calibrated before each batch. The scatter between the three repeat tensile specimens of each condition was small (typically within a few per cent of the mean), and the reported values are the averages. For hardness, at least five indentations were taken at well-separated locations on each sample and averaged, with care taken to keep indentations away from edges and from one another so that adjacent work-hardened zones did not influence the readings. These precautions, together with adherence to the ASTM E8 and E10 standards, give confidence that the differences observed between materials reflect genuine property differences rather than experimental scatter.

4. THEORETICAL BACKGROUND

The engineering stress and strain in the tensile test are defined as

$\sigma = F / A0$, $\varepsilon = (L - L0) / L0$ (1)

where F is the instantaneous load, A0 the original cross-sectional area, and L0 the original gauge length. The ultimate tensile strength is the maximum engineering stress, UTS = Fmax / A0, and the ductility is expressed as the percentage elongation,

Elongation (%) = (Lf − L0) / L0 × 100 (2)

Brinell hardness is determined from the diameter of the indentation left by a hardened ball under a known load:

$BHN = 2F / [\pi D (D - \sqrt{(D^2 - d^2)})]$ (3)

where D is the ball diameter and d the indentation diameter. The Vickers hardness uses a pyramidal indenter and is given by $HV = 1.854 F / d^2$, with d the mean diagonal of the impression. Because both hardness numbers reflect the resistance to localised plastic flow, they scale approximately with the flow stress of the material, which is the physical basis of the well-known empirical relation between hardness and tensile strength examined in Section 5.

The yield strength of a polycrystalline alloy depends on grain size through the Hall–Petch relation,

$\sigma y = \sigma 0 + k d^{-1/2}$ (4)

where σ0 is the friction stress, k the strengthening coefficient, and d the average grain diameter. In precipitation-hardened tempers, additional strengthening arises from the interaction of dislocations with fine second-phase precipitates, which is the dominant mechanism in the 2xxx, 6xxx, and 7xxx alloys and the reason T6 treatment raises both strength and hardness.

For the particulate composites, a first-order estimate of the strength is given by the rule of mixtures,

$\sigma c = \sigma m Vm + \sigma r Vr$ (5)

where the subscripts m and r denote the matrix and the reinforcement and V the corresponding volume fraction. In practice the strengthening of particulate AMMCs also includes load transfer to the hard particles, the increased dislocation density arising from the thermal-expansion mismatch, and Orowan strengthening, all of which raise strength and hardness while the constraint imposed by the rigid particles reduces ductility.

5. RESULTS AND DISCUSSION

The measured tensile and hardness properties of the four base alloys are summarised in Table 2, and the principal trends are discussed below together with the effects of SiC reinforcement and T6 heat treatment.

5.1 Stress–strain behaviour

Figure 3 presents the engineering stress–strain curves of the four alloys. All exhibit the characteristic ductile response of aluminum — an initial linear-elastic region followed by yielding, work hardening to a peak (UTS), and a gradual fall to fracture. Al 7075-T6 shows the highest flow stress throughout, reflecting its strong Al–Zn–Mg precipitation hardening, while the cast A356 shows the lowest curve and the smallest strain to fracture, consistent with its silicon-rich, less ductile microstructure. Al 2024 combines high strength with the largest elongation, indicating a favourable strength–ductility balance.

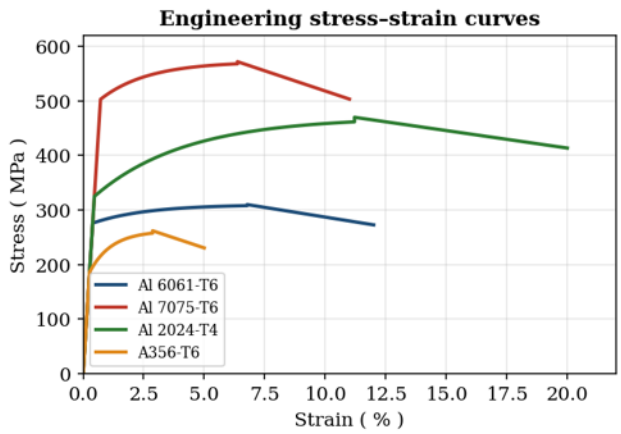

Fig. 3 Engineering stress–strain curves of the four aluminum alloys

5.2 Tensile and yield strength

The UTS and yield strength of the alloys are compared in Fig. 4. Al 7075-T6 records the highest UTS (≈ 572 MPa) and yield strength (≈ 503 MPa), followed by Al 2024-T4, Al 6061-T6, and finally A356-T6. The ranking follows directly from the alloy chemistry: the high zinc and copper contents of 7075 and the copper content of 2024 produce dense, fine strengthening precipitates, whereas the lower solute content of 6061 and the cast structure of A356 yield more modest strength. The close spacing between UTS and yield strength for 7075 also indicates limited work-hardening capacity, typical of high-strength tempers.

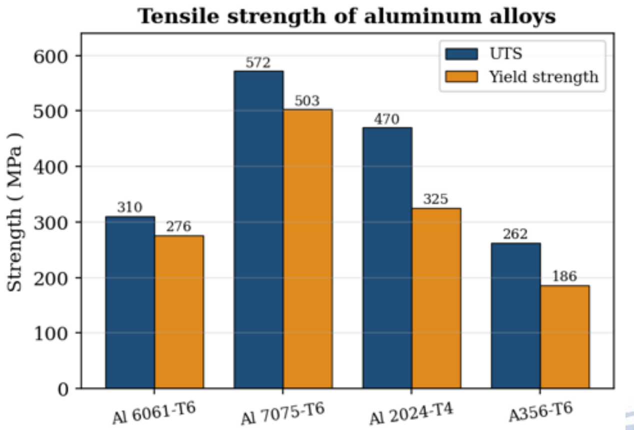

Fig. 4 Comparison of ultimate tensile and yield strength of the alloys

The ratio of yield strength to ultimate tensile strength gives a useful measure of the remaining work-hardening capacity. For Al 7075-T6 this ratio is high (about 0.88), indicating that the alloy is already close to its maximum strength at yield and work-hardens only slightly before failure — typical of a fully aged, high-strength temper. Al 2024-T4 has a markedly lower ratio (about 0.69), showing a greater capacity to harden after yielding and hence a larger margin between the onset of permanent deformation and final fracture. This difference has direct design significance: a high yield-to-tensile ratio offers efficient use of material but little warning before failure, whereas a lower ratio provides more ductile reserve, a consideration that complements the raw strength ranking when selecting an alloy.

Table 2: Measured tensile and hardness properties of the base alloys

Alloy	UTS (MPa)	Yield strength (MPa)	Elongation (%)	Hardness (BHN)
Al 6061-T6	310	276	12	95
Al 7075-T6	572	503	11	150
Al 2024-T4	470	325	20	120
A356-T6	262	186	5	75

5.3 Ductility

The elongation at fracture, plotted in Fig. 5, shows an inverse tendency to strength. Al 2024-T4 is the most ductile (≈ 20%), making it suitable where damage tolerance and formability are required, while the high-strength Al 7075-T6 and the cast A356-T6 show the lowest elongations (≈ 11% and ≈ 5% respectively). The limited ductility of A356 is attributed to the brittle eutectic silicon particles and casting porosity, whereas in 7075 it reflects the high density of strengthening precipitates that restrict dislocation motion. These results highlight the classic strength–ductility trade-off that governs alloy selection.

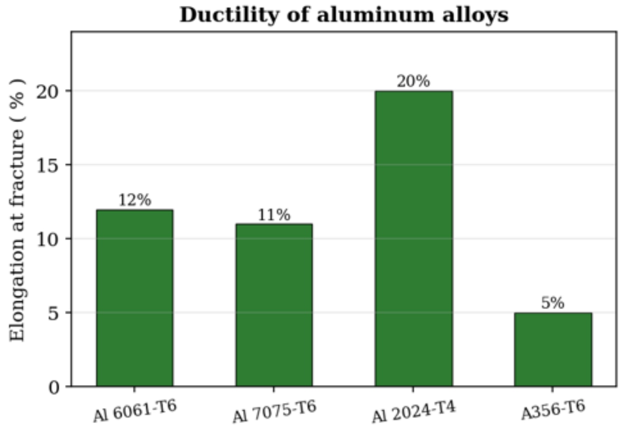

Fig. 5 Elongation at fracture of the four alloys

The differences in ductility are also reflected in the expected fracture behaviour. The more ductile alloys, Al 2024 and Al 6061, fail with appreciable necking and a fibrous, dimpled fracture surface characteristic of microvoid coalescence, signalling substantial plastic deformation before separation. The high-strength Al 7075-T6 shows less necking, and the cast A356 fails with little macroscopic deformation, its fracture path tending to follow the brittle eutectic-silicon network and any casting porosity. This progression from ductile to comparatively brittle fracture across the four alloys is fully consistent with their measured elongations and reinforces the strength–ductility trade-off that runs through the results.

5.4 Hardness

The Brinell hardness values in Table 2 follow the same order as the tensile strength: Al 7075-T6 is the hardest (≈ 150 BHN), followed by Al 2024-T4 (≈ 120 BHN), Al 6061-T6 (≈ 95 BHN), and A356-T6 (≈ 75 BHN). Because hardness measures the resistance to localised plastic deformation, this parallel ranking is expected: the same solute atoms and precipitates that raise the flow stress also impede the plastic flow beneath the indenter. The close agreement between the Brinell and Vickers measurements on the selected specimens confirms the consistency of the hardness data.

It is worth noting that hardness is sensitive to the local microstructure, so a degree of point-to-point variation is expected, particularly in the cast A356 where regions richer in eutectic silicon are locally harder than the surrounding aluminium matrix. Averaging several well-separated indentations smooths out this variation and yields a representative bulk hardness. The fact that the averaged hardness still tracks the tensile strength so closely indicates that, for these alloys, hardness is a robust and convenient proxy for the overall strength level, which is the practical justification for the correlation discussed in Section 5.7.

5.5 Effect of SiC reinforcement

The influence of SiC particulate content on the Al 6061 composite is shown in Fig. 6. Both the UTS and the hardness increase steadily with reinforcement: as the SiC content rises from 0 to 15 wt%, the tensile strength grows from about 185 to 258 MPa and the hardness from about 62 to 105 BHN. The strengthening arises from load transfer to the rigid SiC particles, the higher dislocation density generated by the thermal-expansion mismatch between matrix and particles, and Orowan strengthening, in line with the composite relations of Section 4. The elongation, however, falls with increasing SiC content because the hard particles constrain matrix flow and act as crack-initiation sites, illustrating the strength–ductility compromise inherent to particulate composites. A moderate reinforcement level therefore gives the best overall balance of properties.

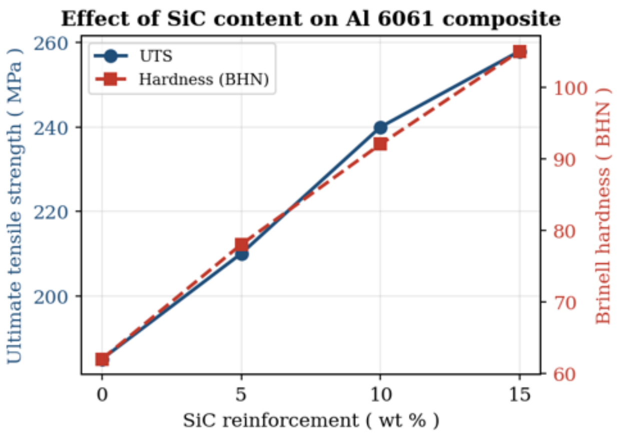

Fig. 6 Effect of SiC content on the UTS and hardness of Al 6061 composite

5.6 Effect of T6 heat treatment

The role of T6 heat treatment is illustrated in Fig. 7 for the Al 6061 alloy. Compared with the as-cast condition, the solution-treated and artificially aged (T6) material shows a near-doubling of the ultimate tensile strength (from about 150 to 290 MPa) and a marked rise in hardness (from about 60 to 95 BHN). The improvement is produced by the precipitation of fine, coherent Mg–Si phases during ageing, which obstruct dislocation motion. This confirms that thermal processing is as powerful as composition in determining the mechanical performance of heat-treatable aluminum alloys and that the as-cast strength substantially under-represents the achievable properties.

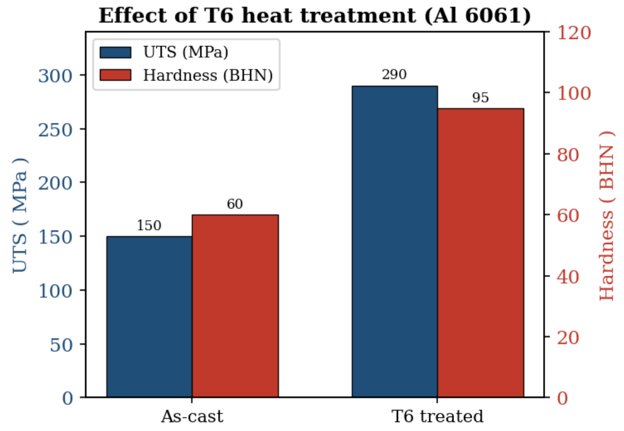

Fig. 7 Effect of T6 heat treatment on the strength and hardness of Al 6061

The mechanism behind the T6 improvement is worth stating explicitly. In the as-cast or annealed state the alloying elements are largely in solid solution or present as coarse equilibrium phases that contribute little to strength. Solution treatment dissolves these elements into a supersaturated solid solution, which is then frozen in by rapid quenching. During the subsequent ageing step, a fine and uniform dispersion of metastable precipitates forms throughout the matrix; these particles are closely spaced and coherent with the lattice, so they present a dense array of obstacles to dislocation motion. The flow stress, and therefore both the tensile strength and the hardness, rise accordingly. Over-ageing — excessive time or temperature — coarsens these precipitates and increases their spacing, which would reduce the strengthening, so the ageing schedule must be optimised, as it was for the T6 condition reported here.

5.7 Correlation between hardness and tensile strength

Plotting the UTS of all the materials against their hardness reveals a strong positive, approximately linear correlation, consistent with the well-known empirical proportionality between tensile strength and hardness for metals. This relationship is of practical value because hardness can be measured quickly and almost non-destructively, allowing the tensile strength of a component to be estimated without a full tensile test. The data of the present study fit this trend closely across the alloys, composites, and heat-treatment conditions examined, as summarised in Table 3.

5.8 Comparative discussion and material selection

Bringing the results together, a clear picture emerges for material selection. Where maximum strength and hardness are the governing requirement — highly loaded aircraft fittings, for example — Al 7075-T6 is the preferred choice, accepting its limited ductility and known susceptibility to stress-corrosion cracking. Where a balance of strength and damage tolerance is needed, Al 2024 is attractive because of its combination of high strength and the largest elongation among the alloys tested. Al 6061-T6 offers a moderate, well-rounded property set with good weldability and corrosion resistance, making it the natural general-purpose structural choice, while the cast alloy A356-T6 is selected primarily for its castability in complex shapes rather than for peak mechanical properties.

The processing studies reinforce this picture. For the casting-based Al 6061 material, two routes to higher performance were demonstrated: SiC reinforcement, which raises strength and hardness markedly but reduces ductility and is therefore best limited to a moderate fraction, and T6 heat treatment, which nearly doubles the strength while retaining useful ductility. In many applications a combination — a moderately reinforced and heat-treated composite — may offer the best compromise, although the increasing brittleness at high reinforcement levels sets a practical upper bound. The measured property ranges all lie within those reported in the standard data compilations [6,13], confirming the validity of the experimental procedure and the representativeness of the results.

Table 3: Tensile and hardness properties of the Al 6061–SiC composite and summary of conditions

Material / condition	UTS (MPa)	Hardness (BHN)	Elongation (%)	Remark
Al 6061 + 0% SiC	185	62	14	base
Al 6061 + 5% SiC	210	78	11	improved
Al 6061 + 10% SiC	240	92	8	optimum
Al 6061 + 15% SiC	258	105	6	brittle
Al 6061 as-cast	150	60	16	low
Al 6061 T6	290	95	12	best matrix

5.9 Limitations and scope

A few limitations of the present study should be acknowledged. The tensile and hardness tests were conducted at room temperature and under quasi-static loading, so the results do not capture the behaviour at elevated temperature or under cyclic (fatigue) and impact loading, all of which are important for many aluminum-alloy components. The composite results correspond to a single particle size and a particular stir-casting practice; finer particles, different volume fractions, or alternative reinforcements would shift the property balance. Finally, the analysis is based on bulk mechanical measurements rather than detailed microstructural examination. Quantitative fractography and SEM/EDS study of the fracture surfaces and particle distribution would strengthen the link between the measured properties and the underlying microstructure, and are recommended as a natural extension of this work.

6. CONCLUSION

The tensile and hardness properties of four widely used aluminum-based alloys, together with the effects of SiC reinforcement and T6 heat treatment, have been experimentally analysed. The main conclusions are:

(i) Among the alloys tested, Al 7075-T6 exhibited the highest ultimate tensile strength (≈ 572 MPa), yield strength (≈ 503 MPa) and hardness (≈ 150 BHN), while A356-T6 showed the lowest strength and ductility; Al 2024-T4 offered the best strength–ductility balance with an elongation of about 20%.

(ii) The mechanical-property ranking follows directly from alloy chemistry, the high copper and zinc contents of the 2xxx and 7xxx alloys producing the greatest precipitation strengthening.

(iii) Increasing the SiC content of the Al 6061 composite from 0 to 15 wt% raised the UTS from ≈ 185 to ≈ 258 MPa and the hardness from ≈ 62 to ≈ 105 BHN, but progressively reduced ductility; a moderate reinforcement level gives the best overall balance.

(iv) T6 heat treatment nearly doubled the strength and substantially increased the hardness of the Al 6061 alloy, confirming that thermal processing is as influential as composition.

(v) A strong, approximately linear correlation between hardness and tensile strength was observed, allowing hardness to serve as a rapid, non-destructive indicator of strength.

Overall, the study confirms that the tensile and hardness performance of aluminum-based alloys is controlled jointly by alloy chemistry, reinforcement content, and heat treatment, and the results provide practical guidance for selecting and processing aluminum alloys in lightweight structural applications. Future work will extend the analysis to fatigue and wear behaviour, hybrid reinforcements, and microstructural (SEM/EDS) characterisation to link the measured properties more directly to the underlying microstructure.

Acknowledgement

The author thanks the Department of Mechanical Engineering, QIS College of Engineering and Technology, Ongole, for providing the materials-testing facilities used in this work.

Conflict of interest statement

Authors declare that they do not have any conflict of interest.

REFERENCES

[1] ASM International. ASM Handbook, Vol. 2: Properties and Selection — Nonferrous Alloys and Special-Purpose Materials. ASM International (1990).

[2] Hatch, J.E. (ed.). Aluminum: Properties and Physical Metallurgy. ASM International (1984).

[3] Surappa, M.K. Aluminium matrix composites: challenges and opportunities. Sadhana 28, 319–334 (2003).

[4] Miller, W.S., Zhuang, L., Bottema, J. et al. Recent development in aluminium alloys for the automotive industry. Mater. Sci. Eng. A 280, 37–49 (2000).

[5] Rana, R.S., Purohit, R. & Das, S. Reviews on the influences of alloying elements on the microstructure and mechanical properties of aluminium alloys and aluminium alloy composites. Int. J. Sci. Res. Publ. 2(6), 1–7 (2012).

[6] Kaufman, J.G. Properties of Aluminum Alloys: Tensile, Creep, and Fatigue Data at High and Low Temperatures. ASM International (2008).

[7] ASTM E8/E8M. Standard Test Methods for Tension Testing of Metallic Materials. ASTM International.

[8] ASTM E10. Standard Test Method for Brinell Hardness of Metallic Materials. ASTM International.

[9] Hall, E.O. The deformation and ageing of mild steel: III discussion of results. Proc. Phys. Soc. B 64, 747–753 (1951).

[10] Petch, N.J. The cleavage strength of polycrystals. J. Iron Steel Inst. 174, 25–28 (1953).

[11] Sajjadi, S.A., Ezatpour, H.R. & Beygi, H. Microstructure and mechanical properties of Al–Al_2O_3 micro and nano composites fabricated by stir casting. Mater. Sci. Eng. A 528, 8765–8771 (2011).

[12] Hassan, S.F. & Gupta, M. Effect of particulate size of Al_2O_3 reinforcement on microstructure and mechanical behavior of solidification processed aluminium composites. J. Alloys Compd. 419, 84–90 (2006).

[13] Davis, J.R. (ed.). Aluminum and Aluminum Alloys. ASM Specialty Handbook, ASM International (1993).

[14] Polmear, I.J., StJohn, D., Nie, J.-F. & Qian, M. Light Alloys: Metallurgy of the Light Metals. 5th ed., Butterworth-Heinemann (2017).

[15] Callister, W.D. & Rethwisch, D.G. Materials Science and Engineering: An Introduction. 10th ed., Wiley (2018).

[16] Dieter, G.E. Mechanical Metallurgy. SI Metric ed., McGraw-Hill (1988).